A Fast Engineering Method for Estimating Iron Losses in Induction Type Motor Spindles Based on Equivalent Magnetic Circuit

Lang Lü (562035363@qq.com)
National Engineering Research Center for High Efficiency Grinding, Hunan University
https://orcid.org/0000-0001-7818-2025
Wanli Xiong
Hunan University
Can Hu
Hunan University of Science and Technology

Original Article

Keywords: Motorized spindle, Iron losses, EMC

Posted Date: June 30th, 2021

DOI: https://doi.org/10.21203/rs.3.rs-655208/v1

ORIGINAL ARTICLE(or REVIEW)

A Fast Engineering Method for Estimating Iron Losses in Induction Type Motor Spindles Based on Equivalent Magnetic Circuit

Lang Lü[1] • Wan-Li Xiong[2] • Can Hu[3]

Received June xx, 201x; revised February xx, 201x; accepted March xx, 201x

Abstract: The iron losses in the motor of motorized spindles have a significant effect on the heat generation, working efficiency, and speed-torque characteristics of motorized spindles as well as on their thermal deformation and machining accuracy. The existing finite element and analytical methods based on Maxwell's equations are too complicated to be suitable for engineering designers. A fast engineering method for estimating iron losses in the spindle motor is presented based on equivalent magnetic circuit (EMC) where the problem of solving a complex electromagnetic field inside the spindle motor is simplified into a simple magnetic circuit calculation by the assumption that the magnetic flux density distribution of any cross section along the magnetic flux direction in the spindle motor is uniform. The EMC is combined with the Boglietti's model. They are integrated into a developed program by compiling source codes to achieve the analysis and prediction of iron losses in the spindle motor. The results obtained from the proposed method are compared with the prototype experiment data to verify its validity. With the purpose of ensuring accurate experiment results of iron losses, a method of no load running combined with a sudden loss of power supply is proposed to eliminate the braking torque and electromagnetic losses of the spindle motor, namely to achieve the separation of the mechanical loss from the total losses.

Keywords: Motorized spindle • Iron losses • EMC

✉ Lang Lü
562035363@qq.com
[1] Hunan Provincial Engineering Laboratory of Wind Power Operation, Maintenance and Testing Technology, Hunan Institute of Engineering, Xiangtan 411104, China

[2] National Engineering Research Center for High Efficiency Grinding, Hunan University, Changsha 410082, China

[3] School of Mechanical Engineering, Hunan University of Science and Technology, Xiangtan 411201, China

1 Introduction

Motor or Motorized spindles belong to a new kind of machine tool spindles, where middle transmission chains like belts or gears are cancelled, namely achieving zero transmission chain or direct drive. They have prominent advantages over traditional mechanical spindles, e.g., compact structure, small inertia, fast dynamic response, high speed (high productivity), high precision, wide speed range, low vibration and noise, and easy to realize automatic and precise control [1]-[3]. Motorized spindles have been increasingly applied to high speed precision machining such as high speed milling, high speed grinding, high speed turning, and high speed drilling [4]-[5].

Induction motors (IMs) are more popularly chosen as a drive motor of motorized spindles than permanent magnet synchronous motors (PMSMs) because they have simple and reliable rotor structure, no rotor demagnetization, and high performance-price ratio. As a drive motor of motorized spindles, IMs are always fed by a voltage source inverter. The output voltage waveform of the inverter is not a sinusoidal wave but a series of rectangular pulse waves [6]-[7]. Numerous harmonic components from inverter supply are introduced into the stator winding current of the spindle motor. This makes the iron losses of the spindle motor in their physical origins more complicated. It is a challenge task to analyze and predict them accurately. The calculation results of motorized spindles such as heat generation, thermal deformation [8]-[9], and working efficiency are further affected when motorized spindles are developed and designed. Therefore, to find a fast and accurate prediction method of iron losses in the spindle motor is very important for reducing the development and

design cost of motorized spindles, and improving their performance.

The ongoing study of iron losses in motors has been done because of their complex generation mechanisms [10]-[12]. The proper modeling of soft magnetic materials (SMMs) is the basis of performing the exact analysis and prediction of iron losses in motors. There are two basic types of loss models. One type is frequency domain model and the other type is time domain model.

Various frequency domain models have been developed [13]-[18]. Bertotti [14] proposed a three-term loss separation model based on the Steinmetz's equation [13], in which the additional power consumption during a magnetization process of SMMs due to domain wall effect is considered, and the total losses can be expressed as a three-term sum of the hysteresis loss, the classical eddy current loss, and the excess loss. However, the Steinmetz's equation and the Bertotti's model can achieve satisfactory accuracies within a certain range of magnetic flux density levels and frequencies. Moreover, they are valid for only sinusoidal magnetic flux waveform excitation.

Boglietti et al [15]-[16] presented a general loss model according to the fact that any loss component contribution in it depends on the characteristics of supply voltage and the Bertotti's model [14]. The Boglietti's model is suitable for any voltage waveform supply. On the basis of the Boglietti's model, variable parameter models [17]-[18], where the hysteresis and eddy current loss coefficients are assumed as the functions of the magnitude and frequency of the magnetic flux density, were investigated for obtaining more accurate results over wide frequency and magnetic flux density ranges, but they need more experiment data to extract the model parameters before use.

Besides various frequency domain models, different time domain models have also been developed. Reinert et al [19] investigated a modified Steinmetz's equation (MSE) in time domain to estimate the loss in SMMs under arbitrary flux waveforms. In time domain, Barbisio et al [20] developed a general loss model of SMMs with regard for minor hysteresis loops. However, the modeling [19]-[20] is to model the magnetic characteristics of SMMs in the case of only an alternating magnetic field.

In order to describle the hysteresis phenomena and magnetic properties of SMMs under both rotating and alternating fields, a generalized vector hysteresis model [21]-[22] in time domain was established from a traditional Chua-type vector hysteresis model [23]. A comparison study between frequency and time domain models was made to predict the excess loss [24].

Time domain models [19]-[24] can gain better accuracy than frequency domain models [13]–[18] because of considering more realistic situations such as magnetic saturation, hysteresis properties, magnetic field rotating and alternating, and distorted magnetic flux waveforms. However, they require extensively experimental tests to construct the database of the model parameters. In addition, they are always combined with the finite element to use.

The combination of the finite element analysis (FEA) and the loss models of SMMs has become a fashionable method of calculating iron losses in motors [8], [25]-[29]. The FEA is used along with the Bertotti's model to estimate iron losses in a slot-less PMSM with the stator cores made from two different types of SMMs [8], and together with the MSE to calculate the hysteresis loss in a surface-mounted PMSM [27]. The desired or accurate results can be obtained from the FEA, but it requires a long enough time for the preparation work including motor modelling, model meshing, and material definition. Also the computation is time-consuming. The analytical method based on Maxwell's equations was studied to improve computational efficiency [30]-[31]. However, both FEA and analytical methods based on Maxwell's equations are too complicated to be suitable for engineering designers.

In this paper, a fast engineering method to estimate iron losses in the spindle motor is proposed based on equivalent magnetic circuit (EMC), where the problem of solving a complex electromagnetic field inside the spindle motor is simplified into a simple magnetic circuit calculation by assuming that the magnetic flux density distribution of any cross section along the magnetic flux direction in the spindle motor is uniform. The EMC is used together with the Boglietti's model to realize the analysis and prediction of iron losses in the spindle motor. The validity of the proposed method is proved by prototype experiment.

2 Iron Loss Model

2.1 Model under Sinusoidal Flux Excitation

It is well known that a classical model is the Bertotti's three-term loss separation model [14], in which the total losses are divided into three components: the hysteresis loss, the classical eddy current loss, and the excess loss. The model can be expressed by a mathematical formula as

$$P = P_{\mathrm{h}} + P_{\mathrm{ec}} + P_{\mathrm{e}} \tag{1}$$

Where P denotes the total losses. P_{h}, P_{ec} and P_{e} are the respective hysteresis, classical eddy current, and excess losses.

The power consumption or hysteresis loss inside

electrical steel sheets (ESSs) is generated by a change in the direction of a magnetic field applied to them. The hysteresis loss can be formulated as

$$P_{\mathrm{h}} = afB_{\mathrm{p}}^{x} \tag{2}$$

Where a represents the hysteresis loss coefficient related to magnetic material properties, f is a magnetic field frequency, B_{p} is the peak value of the magnetic flux density, and x denotes the Steinmetz coefficient.

The classical eddy current loss is resulted from that ESSs are incised by a rotating magnetic field to induce an electromotive force (EMF). The eddy currents inside ESSs are formed with an induced EMF and the subsequent Joule heat is produced. The classical eddy current loss can be formulated as

$$P_{\mathrm{ec}} = bf^{2}B_{\mathrm{p}}^{2} \tag{3}$$

Where b represents the classical eddy current loss coefficient and it is formulated as

$$b = \frac{\sigma\pi^{2}d^{2}}{6\rho} \tag{4}$$

Where σ, d and ρ are the electrical conductivity, the thickness, and the density of soft magnetic materials (SMMs).

The additional power consumption or excess loss is caused by domain wall effect during a magnetizing process of SMMs. The excess loss can be characterized by a formula as

$$P_{\mathrm{e}} = ef^{1.5}B_{\mathrm{p}}^{1.5} \tag{5}$$

Where e denotes the excess loss coefficient.

If the term of the excess loss in (1) is ignored then (1) can be reduced to

$$P = P_{\mathrm{h}} + P_{\mathrm{ec}} \tag{6}$$

The ignored term of the excess loss is actually included in the other two terms: the hysteresis loss and the classical eddy current loss [15]-[16].

Equations (2) and (3) are substituted into (6), then

$$P = afB_{\mathrm{p}}^{x} + bf^{2}B_{\mathrm{p}}^{2} \tag{7}$$

Formula (7) is valid for only sinusoidal flux waveform excitation. The unit of the results calculated from (7) is expressed in W/kg.

2.2 Model with Inverter Supply

The Boglietti's model is a representative loss model of SMMs with inverter supply [15]. In the model, minor hysteresis loops are usually neglected because of high inverter switching frequency and the additional harmonic eddy current losses due to inverter supply are taken into consideration by a model correction factor (MCF). The model can be expressed by a formula as

$$P_{\mathrm{PWM}} = \overbrace{\underbrace{afB_{\mathrm{p}}^{x}}_{P_{\mathrm{h}}} + \underbrace{bf^{2}B_{\mathrm{p}}^{2}}_{P_{\mathrm{ec}}}}^{\text{Total fundamental losses}} + \underbrace{\left(\chi^{2}-1\right)\overbrace{bf^{2}B_{\mathrm{p}}^{2}}^{P_{\mathrm{ec}}}}_{\text{Total harmonic losses}} \tag{8}$$

Where χ^{2} ($\chi \geq 1$) is the MCF, χ denotes the ratio between the root mean square value of the total voltage from inverter supply and that of its fundamental voltage. On the right side of (8), the sum of the first two terms stands for the total fundamental losses and the last term represents the total harmonic losses.

3 Equivalent Magnetic Circuit

In order to simplify the problem of solving a complex electromagnetic field inside motors into a simple magnetic circuit calculation, it is assumed that the magnetic flux density distribution of any cross section along the magnetic flux direction in motors is uniform. A typical magnetic circuit of induction motors (IMs) per pole is shown in Figure 1.

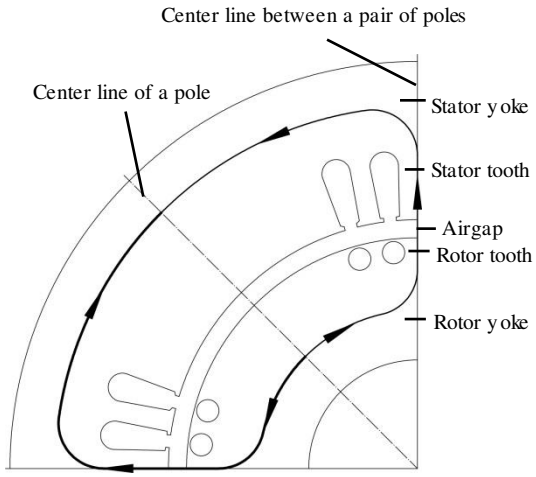

Figure 1 Typical magnetic circuit of IMs per pole

According to Ampere's loop law, the integral result is independent of the path. A magnetic circuit which passes through the center line between two adjacent or a pair of magnetic poles is usually chosen as one for calculation, as illustrated in Figure 1. The magnetic circuit consists of five parts: airgap, stator tooth, stator yoke, rotor tooth, and rotor yoke segments. Only one half of the magnetic circuit is calculated because of its symmetry.

The magnetic flux of IMs per pole can be calculated from the following formula [32]

$$\Phi = \frac{E}{2.22 f N_\phi K_{\mathrm{dp}}} \tag{9}$$

Where E is an induced winding back electromotive force (BEMF) per phase, f is a power supply frequency, N_ϕ denotes the number of stator winding series conductors per phase, and K_{dp} is a stator winding coefficient which depends on the number of slots per pole per phase, the electrical angular degree between two adjacent slots, and the number of slots spanned by two effective sides of a winding coil.

The peak value of the magnetic flux density in airgap can be obtained from a mathematical expression [32] as

$$B_{\delta,\mathrm{p}} = F_{\mathrm{s}} \frac{\Phi}{\tau l_{\mathrm{ef}}} \tag{10}$$

Where F_{s} is the waveform amplitude coefficient of the magnetic flux density in airgap (the ratio of the peak value of the magnetic flux density in airgap to its average value) and it is a function of magnetic saturation occurring in stator and rotor core teeth, τ is the pole pitch expressed in that the circumference of a circular inner hole of the stator core is divided by the number of poles, and l_{ef} denotes an effective core length.

The respective calculation formulas of the magnetic flux densities of stator and rotor teeth can be expressed as

$$B_{\mathrm{st,p}} = F_{\mathrm{s}} \frac{\Phi}{A_{\mathrm{st}}} \tag{11}$$

$$B_{\mathrm{rt,p}} = F_{\mathrm{s}} \frac{\Phi}{A_{\mathrm{rt}}} \tag{12}$$

Where $B_{\mathrm{st,p}}$ and $B_{\mathrm{rt,p}}$ are the respective peak values of the magnetic flux densities of stator and rotor teeth, A_{st} and A_{rt} represent the respective sums of the flux areas of stator and rotor teeth per pole, $A_{\mathrm{st}} = b_{\mathrm{st}} Z_1 / (2p) l_{\mathrm{s}}$ and $A_{\mathrm{rt}} = b_{\mathrm{rt}} Z_2 / (2p) l_{\mathrm{r}}$. Where b_{st} and b_{rt} are the respective widths of stator and rotor teeth, Z_1 and Z_2 are the respective numbers of stator and rotor slots, p is the number of pole pairs, l_{s} and l_{r} denote the respective net lengths of the laminated stator and rotor cores, $l_{\mathrm{s}} = K_{\mathrm{Fe}} l_1$ and $l_{\mathrm{r}} = K_{\mathrm{Fe}} l_2$. Where K_{Fe} is a laminated coefficient, l_1 and l_2 are the respective lengths of the laminated stator and rotor cores.

The magnetic flux densities of different yoke cross sections along the magnetic flux direction are not same. When a yoke cross section passes through the center line between two adjacent poles, the magnetic flux density of the section reaches its maximum value, but when a yoke cross section passes through the center line of a pole, the magnetic flux density of the section is exactly equal to zero, as shown in Figure 1. Thus, the total magnetic flux of yoke parts is only one half of the magnetic flux per pole. The maximum magnetic flux densities of stator and rotor yoke parts can be formulated respectively as

$$B_{\mathrm{sj,p}} = \frac{1}{2} \frac{\Phi}{A_{\mathrm{sj}}} \tag{13}$$

$$B_{\mathrm{rj,p}} = \frac{1}{2} \frac{\Phi}{A_{\mathrm{rj}}} \tag{14}$$

Where A_{sj} and A_{rj} are the respective flux areas of stator and rotor yoke parts, $A_{\mathrm{sj}} = h'_{\mathrm{sj}} l_{\mathrm{s}}$ and $A_{\mathrm{rj}} = h'_{\mathrm{rj}} l_{\mathrm{r}}$. Where h'_{sj} and h'_{rj} are the respective calculation heights of stator and rotor yokes, and they are commonly determined by their geometrical yoke heights together with slot types.

4 Calculation of Iron Losses in Spindle Induction Motors

The equivalent magnetic circuit (EMC) is combined with (8) to estimate iron losses in induction motors (IMs) of motorized spindles. The spindle motor is supplied with a voltage source inverter. The EMC is used to calculate the magnetic flux densities of the spindle motor stator and rotor cores and the corresponding loss densities are calculated by (8). The total iron losses in the spindle motor can be calculated from the following formula

$$P_{\mathrm{Fe}} = \overbrace{K_1 m_{\mathrm{st}} P_{\mathrm{PWM}}\left(B_{\mathrm{st,p}}, f\right) + K_2 m_{\mathrm{sj}} P_{\mathrm{PWM}}\left(B_{\mathrm{sj,p}}, f\right)}^{\text{Iron losses in the stator core}} + \underbrace{K_1 m_{\mathrm{rt}}\left(\chi^2 - 1\right) P_{\mathrm{ec}}\left(B_{\mathrm{rt,p}}, f\right) + K_2 m_{\mathrm{rj}}\left(\chi^2 - 1\right) P_{\mathrm{ec}}\left(B_{\mathrm{rj,p}}, f\right)}_{\text{Iron losses in the rotor core}} \tag{15}$$

Where K_1 and K_2 are empirical coefficients to consider rotor rotating motion combined with tooth and slot effect, $P_{\mathrm{PWM}}\left(B_{\mathrm{st,p}}, f\right)$ and $P_{\mathrm{PWM}}\left(B_{\mathrm{sj,p}}, f\right)$ are the loss densities of the tooth and yoke parts of the stator core, $\left(\chi^2-1\right)P_{\mathrm{ec}}\left(B_{\mathrm{rt,p}}, f\right)$ and $\left(\chi^2-1\right)P_{\mathrm{ec}}\left(B_{\mathrm{rj,p}}, f\right)$ are the loss densities of the tooth and yoke parts of the rotor core, m_{st}, m_{rt}, m_{sj}, and m_{rj} are the total masses of the tooth and yoke parts of stator and rotor cores, where $m_{\mathrm{st}}=\rho b_{\mathrm{st}} h'_{\mathrm{st}} Z_1 l_{\mathrm{s}}$, $m_{\mathrm{rt}}=\rho b_{\mathrm{rt}} h'_{\mathrm{rt}} Z_2 l_{\mathrm{r}}$, $m_{\mathrm{sj}}=\rho\pi\left(D_1-h'_{\mathrm{sj}}\right)h'_{\mathrm{sj}} l_{\mathrm{s}}$, and $m_{\mathrm{rj}}=\rho\pi\left(D_{\mathrm{i2}}+h'_{\mathrm{rj}}\right)h'_{\mathrm{rj}} l_{\mathrm{r}}$. Where ρ is the density of ESSs, h'_{st} and h'_{rt} are the stator and rotor tooth calculation lengths used for magnetic circuit calculating and they are related to slot types but the notch heights of slots are usually ignored in them, D_1 and D_{i2} denote the outer and inner diameters of stator and rotor cores.

In (15), both fundamental and harmonic components from inverter supply are significant contributors to iron losses in the stator core. However, there is almost no contribution of the fundamental component from inverter supply to iron losses in the rotor core owing to a very small rotor slip. The iron losses in the rotor core are mainly caused by the harmonic components from inverter supply. These may explain why the loss densities of stator and rotor cores are different.

The proposed calculation method of iron losses in the spindle motor is integrated into a developed program [33] by compiling source codes. The detailed calculation processes of the developed program are shown in Figure 2.

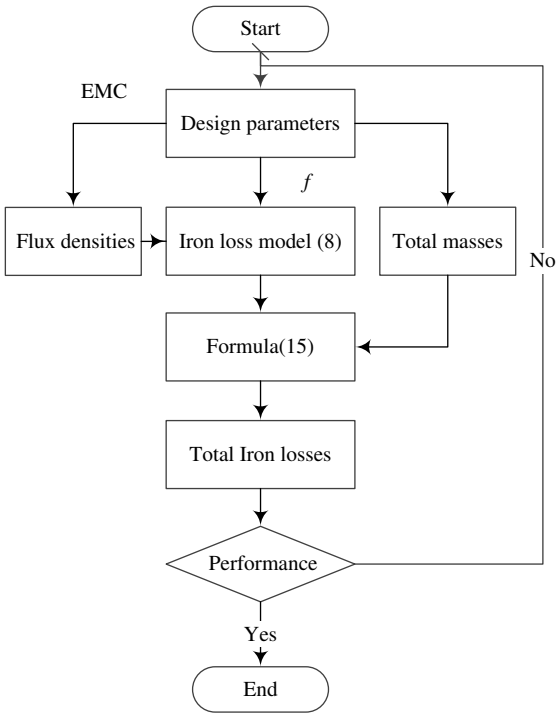

Figure 2 Calculation of iron losses in the spindle motor

STEP1: The data of the spindle motor design parameters, e.g., voltage, frequency, shaft power, the number of pole pairs, and geometrical dimensions are input to the developed program before its run.

STEP2: The magnetic flux density levels of airgap, stator and rotor cores can be calculated from the EMC and the known values of the design parameters.

STEP3: The loss densities of the tooth and yoke parts of stator and rotor cores are obtained from (8), the magnetic flux density levels calculated from STEP 2, and a known inverter supply frequency. There is need for determining the loss coefficients in (8) from the physical characteristic and experimental data of ESSs before model use.

STEP4: The total masses of the tooth and yoke parts of stator and rotor cores are calculated from their structures, and the corresponding geometrical dimensions and material densities.

STEP5: The total iron losses of the spindle motor are divided into two parts: static and dynamic iron losses. The static iron losses in the spindle motor are produced due to magnetic field alternating. They can be expressed as a sum of multiplying the total masses of the tooth and yoke parts of stator and rotor cores by the corresponding loss densities.

STEP6: The dynamic iron losses in the spindle motor are caused by rotor rotating motion combined with tooth and slot effect. They are commonly taken into account based on the static iron losses by introducing empirical coefficients (whose values are always more than 1) because of their complex generation mechanisms.

STEP7: The total iron losses can be calculated and obtained according to (14), the results of the total masses of the tooth and yoke parts of stator and rotor cores and the corresponding loss density values calculated from STEPs 3 and 4

STEP8**:** The calculation will be not stopped until the performance requirements of the spindle motor are satisfied. The performance of the spindle motor can be optimized by changing design parameters.

5 Study Case

5.1 Spindle Motor

The spindle motor taken as a study case is a three-phase inverter-fed induction motor. The performance parameter values of the spindle motor are calculated and obtained from the developed program [33], as seen in Table 1.

Table 1 Specifications of the spindle motor

Parameters	Values
Number of pole pairs	2
Rated voltage	380 V
Rated power	35 kW
Rated synchronous speed	6 000 r/min
Rated current	67 A
Rated efficiency	86.4 %
Rated power factor	0.92
Number of stator and rotor slots	48/38
Stator outer diameter	160 mm
Stator inner diameter	110 mm
Rotor outer diameter	109.1 mm
Rotor inner diameter	78 mm
Laminated core length	230 mm
Air gap length	0.45 mm
Stator resistance per phase (@115℃)	0.1 077 Ω
Rotor resistance per phase (@115℃)	0.1 273 Ω
Stator leakage reactance per phase	0.3 940 Ω
Rotor leakage reactance per phase	0.4 302 Ω
Excitation reactance per phase	19.0 967 Ω

Figure 3 shows the laminated sheets of the stator and rotor cores of the spindle motor.

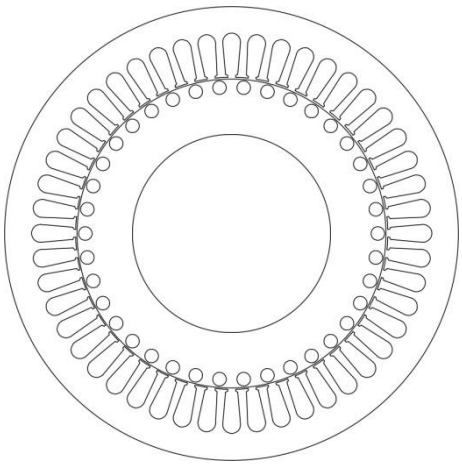

Figure 3 Laminated sheets of stator and rotor cores

The respective slot types of stator and rotor laminated sheets are designed as pear and circle slots. The laminated sheets of stator and rotor cores have 48 and 38 slots, respectively. All the slots are uniformly distributed in their own circumferential directions.

A slot number combination of 48 and 38 is the combination in which there is an obvious difference between stator and rotor slot numbers to reduce electromagnetic vibration and noise. The slot number of the stator laminated sheet is designed as 48. It belongs to a more slot design to obtain a smaller stator outer diameter and more compact stator structure, and to suppress slot harmonic losses and asynchronous additional torque.

The bars in a rotor cage of the spindle motor are designed as copper ones to reduce rotor heat generation and slip, and to improve efficiency as illustrated in Figure 4 b.

(a) Stator (b) Rotor

Figure 4 Stator and rotor manufactured and fabricated

35W300 ESSs are chosen to manufacture and fabricate the stator and rotor cores of the spindle motor to suppress eddy currents and reduce magnetizing current because of their thin thicknesses and high permeability, as shown in Figure 4 a and b. The properties of 35W300ESSs are given in Table 2.

Table 2 Physical and magnetic properties of 35W300 ESSs

Thickness d (mm)	0.35
Density ρ (kg/m^3)	7, 650
Electrical conductivity σ ($\Omega^{-1}\cdot m^{-1}$)	3.75×10^6
Specific loss @ 50 Hz and 1.6 T(W/kg)	3.00
Minimum magnetic density @ 2 500 A/m (T)	1.55
Minimum magnetic density @ 5 000 A/m (T)	1.65
Minimum magnetic density @ 9 800 A/m (T)	1.76

5.2 Model Parameter Extraction

The fundamental parameters in (8) are composed of the hysteresis coefficient a, the Steinmetz coefficient x, and the classical eddy current coefficient b. They can be extracted from the physical characteristic and experimental data of 35W300 ESSs before model use. In the case of sinusoidal flux waveform excitation, the value of the parameter χ in (8) is equal to 1. The Steinmetz coefficient x is assumed as a constant value of 2 because the desired results of iron losses in motors can be achieved [34]-[35]. The value of the parameter b is calculated and obtained from (4) and the known physical characteristic data of 35W300 ESSs (Table 2). Base on

the measured data of 35W300 ESSs under 50 Hz sinusoidal excitation, (8) is fitted by the least square to obtain the value of the parameter a. As a result, the values of the fundamental parameters in (8) are given in Table 3.

Table3 Model parameters and the corresponding values

Hysteresis coefficient a ($W{\cdot}kg^{-1}{\cdot}Hz^{-1}{\cdot}T^{-2}$)	0.0 178
Steinmetz coefficient x	2
Eddy current coefficient b ($W{\cdot}kg^{-1}{\cdot}Hz^{-2}{\cdot}T^{-2}$)	0.0 000 988

6 Experiment

The mechanical loss separation and measurement, and iron loss test are performed on a developed and manufactured motor spindle prototype (Figure 5) which is supported by hydrostatic bearings. The rated power and rotational speed of the prototype are 35 kW and 6, 000 r/min, respectively.

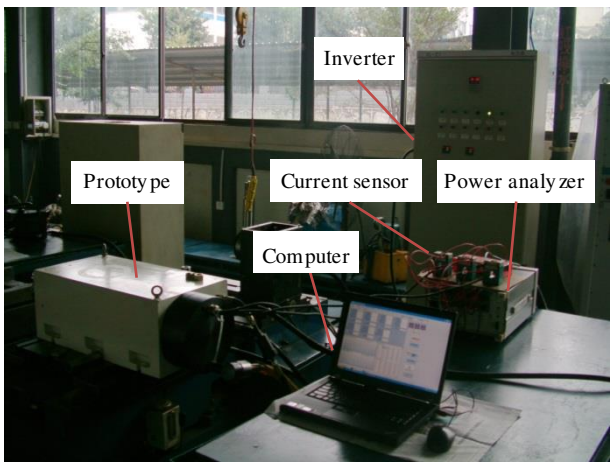

Figure 5 Testing of the prototype

The specifications of the prototype motor are exactly the same as those of the spindle motor in Table 1. The prototype works under the condition of inverter power supply.

6.1 Mechanical Loss Separation and Measurement

The mechanical loss is a major loss of the prototype. Whether it can be correctly separated from the total losses of the prototype by experiment or not will affect the credibility of the experimental results of iron losses.

The mechanical loss of the prototype resulted from bearing friction and rotor wind drag is assumed as a function of its rotational speed square

$$P_{\mathrm{m}} = c\omega_{\mathrm{m}}^2 \tag{16}$$

Where P_{m} denotes the mechanical loss of the prototype running at any speed, c is the rotor rotating friction factor, and ω_{m} is the mechanical angular velocity of the prototype rotor.

The no load running is combined with sudden power cut to separate the mechanical loss of the prototype from the total losses. The inverter-fed prototype is started under no load and its speed rises to a rated speed of 6 k r/min by changing inverter supply frequency. Under no load, the prototype is kept running at the rated speed for a long enough time so that the temperature rise of the prototype is not changed any more. When the temperature rise is stable, the power supply of the prototype is suddenly cut off to eliminate the braking torque and electromagnetic losses of the prototype to obtain accurate test results. In other word, only the mechanical loss is left. After a sudden loss of power supply, the speed of the prototype will not decrease to zero immediately but show a drop process due to frictional forces. The mechanical loss of the prototype can be measured by measuring the rotor rotating friction factor of the prototype and its mechanical rotational speed, as seen in (16).

It is known from the conservation law of energy that under the condition of suddenly losing power supply, the loss of kinetic energy of the prototype in any time interval is exactly equal to the work done to overcome frictional forces in this time interval. The conservation equation of energy is written as

$$-\int_{t_1}^{t_2} P_{\mathrm{m}}\mathrm{d}t = E_{\mathrm{k2}} - E_{\mathrm{k1}} = \frac{1}{2}J\left(\omega_{\mathrm{m2}}^2 - \omega_{\mathrm{m1}}^2\right) \tag{17}$$

Where t_1 and t_2 denote two different rotating motion moments of the prototype after sudden power cut and they can be measured by a stopwatch, E_{k1} and E_{k2} are the kinetic energy of the prototype at the moments t_1 and t_2, J is the total moment of inertial of the prototype rotor including a motor rotor, and a shaft and its accessories, which can be calculated from rotor structures, and the corresponding dimensions and material densities (J=0.0 583 $\mathrm{kg{\cdot}m^2}$), ω_{m1} and ω_{m2} are the measured mechanical angular velocities of the prototype rotor at the moments t_1 and t_2 by using a rotational speed meter.

After a sudden loss of power supply, the mechanical

angular velocity of the prototype rotor is assumed as a polynomial

$$\omega_{\mathrm{m}}(t) = c_0 t^3 + c_1 t^2 + c_2 t + c_3 \tag{18}$$

Where t and ω_{m} denote any moment of the prototype after sudden power cut and the corresponding rotor mechanical angular velocity. c_0, c_1, c_2 and c_3 are the polynomial coefficients.

The measured data of a rotational speed change in the prototype after sudden power cut are listed in Table 4.

Table 4 Measured results of a speed change in the prototype

Speed 1 at $t_1 = 0$ (k r/min)	Speed 2 at t_2 (k r/min)	Av. time required from speed 1 to speed 2 (s)
6	5	1.35
6	3	5.08
6	1	12.50

Based on the measured data in Table 4, (18) is combined with (16) and (17) to solve the value of the rotor rotating friction factor, namely $c = 0.0080$ $\mathrm{N \cdot m \cdot s \cdot rad^{-1}}$.

6.2 Iron Loss Test

A simpler method is used to measure iron losses in the prototype than the traditional method, where there is no need for connecting the prototype under test to a synchronous motor with the same pole pairs. The no load active power of the prototype rotating at different speeds is measured by a power analyzer. The current of the no load operating prototype at any speed exceeds a power analyzer current limit value of 5 A. Thus, current sensors are required in the test. The current sensors with a transformer ratio of 1:40 can be chosen from a power capacity of the prototype.

The iron losses in the prototype can be indirectly obtained from the following formula

$$P_{\mathrm{ir}} = P_{\text{no-load}} - P_{\mathrm{m}} - mR_{\mathrm{s}}I_{\mathrm{s}}^2 \tag{19}$$

Where P_{ir} denotes the total iron losses, $P_{\text{no-load}}$ is the measured no load active power, P_{m} is the measured mechanical loss, m is the number of phase, R_{s} and I_{s} are the measured respective winding resistance and current per phase.

In (19), both stray and rotor resistance loss terms are neglected, but they are included in the total iron losses. The term of the stray loss at no load is very small so that it can be ignored. The term of the rotor resistance loss can also be ignored because of a very low rotor slip at no load. The good measurement accuracy can be still guaranteed even without considering them.

7 Results and Discussion

Figure 6 shows the measured results of various losses of the no load running prototype at different speeds.

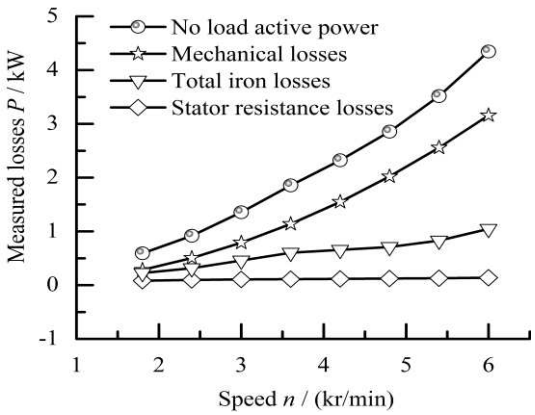

Figure 6 Experimental curves of various losses of the prototype under no load

Figure 7 shows a comparison between the theoretical and experimental curves of iron losses in the prototype under no load.

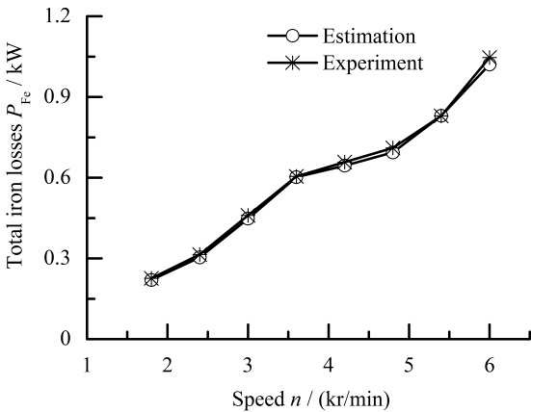

Figure 7 Comparison between the estimated and measured results of iron losses in the prototype at no load

It can be found from Figure 6 that in no exceeding the rated speed range, the total iron losses in the prototype increase with an increase in its rotational speed. The reasons are summarized in two aspects. First, a *V/f* control strategy is adopted to keep the magnetic flux of the prototype constant within a rated speed range, but the static iron losses in the prototype due to magnetic field alternating are increased with a higher rotational speed or magnetic field frequency. Second, the dynamic iron losses in the prototype increase with an increase in the rotational speed because of rotor rotating motion combined with tooth and slot effect.

It can be known from Figure 7 that the results obtained from the proposed method agree well with the prototype experiment data. The biggest error between the estimated and measured results is no more than 10 %. The validity of the proposed method is confirmed by experiment.

The proposed method is simpler and more suitable for engineering designers than the FEA and analytical methods based on Maxwell's equations. In the proposed method, there is no need to solve a complex electromagnetic field inside motors, and to perform 2D or 3D eddy current analysis and the corresponding post-processing.

8 Conclusions

(1) A fast Engineering method for estimating iron losses in the inverter-fed induction motor of motorized spindles is presented based on equivalent magnetic circuit (EMC), in which the EMC is combined with the Boglietti's model and they are integrated into a developed program by compiling source codes to realize the analysis and prediction of iron losses in the spindle motor.

(2) The proposed method is simpler and more suitable for engineering designers than the FEA and analytical methods based on Maxwell's equations because it does not need to solve a complex electromagnetic field inside motors.

(3) The results obtained from the proposed method are compared with the prototype experiment data to verify its validity. It is demonstrated that the biggest error between the calculated and measured results is no more than 10%. The proposed method is valid for analyzing and predicting iron losses in the spindle motor and it can provide technical support for the analyses of the heat generation, working efficiency, and speed-torque characteristics of motorized spindles as well as those of their thermal deformation and rotating error when motorized spindles are developed and designed.

(4) A method of no load running combined with a sudden loss of power supply to separate and measure the mechanical loss of induction type motor spindles is proposed. The proposed method can eliminate the braking torque and electromagnetic losses of the spindle motor, and can achieve the separation of the mechanical loss from the total losses.

9 Declaration

Funding

Supported by National Natural Science Foundation of China (Grant No.), Grant Fund of Newly Introduced PhDs of Hunan Institute of Engineering, and Open Fund of Provincial Key Laboratory of High Efficiency and Precision Machining of Difficult to Cutting Materials of Hunan University of Science and Technology of China (Grant No.E21534)

Availability of data and materials

The datasets supporting the conclusions of this article are included within the article.

Authors' contributions

The authors' contributions are as follows: Lang Lü wrote the manuscript and finished all experimental and theoretical analyses; Wan-Li Xiong gave suggestions for manuscript improvement; Can-Hu read the manuscript and improved the manuscript expression.

Competing interests

The authors declare no competing financial interests.

Consent for publication

Not applicable

Ethics approval and consent to participate

Not applicable

References

[1] Zinan Wang, Ke Zhang, Zhan Wang, et al. Research on vibration of ceramic motorized spindle influenced by interference and thermal displacement. *Journal of Mechanical Science and Technology*, 2021, 35 (6): 2325-2335.

[2] Changjiang Zhou, Zefeng Qu, Bo Hu, et al. Thermal network model and experimental validation for a motorized spindle including thermal–mechanical coupling effect. *The International Journal of Advanced Manufacturing Technology*, 2021, 115: 487-501.

[3] Yanbing Ni, Biao Zhang, Yupeng Sun, et al. Accuracy analysis and design of A3 parallel spindle head. *Chinese Journal of Mechanical Engineering*, 2016, 29: 239-249.

[4] A Y Barbin, V V Molodtsov. Motorized spindles as primary drives in metal-cutting machines. *Russian Engineering Research*, 2013, 33(8): 16-21.

[5] E Abele, Y Altintas, C Brecher. Machine tool spindle units. *CIRP Annals-Manufacturing Technology*, 2010, 59(2): 781-802.

[6] A Krings, J Soulard, O Wallmark. PWM influence on the iron losses and characteristics of a slotless permanent-magnet motor with SiFe and NiFe stator cores. *IEEE Transactions on Industry Applications*, 2015, 51(2): 1475-1484.

[7] A Boglietti, P Ferraris, M Lazzari. Change of the iron losses with the switching supply frequency in soft magnetic materials supplied by PWM inverter. *IEEE Transactions on Magnetics*, 1995, 31(6): 4250-4252.

[8] Yang Liu, Xiaofeng Wang, Xiaogang Zhu, et al. Thermal error prediction of motorized spindle for five-axis machining center based on analytical modeling and BP neural network. *Journal of Mechanical Science and Technology*, 2021, 35 (1): 281-292.

[9] Qianjian Guo, Shuo Fan, Rufeng Xu, et al. Spindle thermal error optimization modeling of a five-axis machine tool. *Chinese Journal of Mechanical Engineering*, 2017, 30: 746-753.

[10] K Yamazaki, Y Kato. Iron loss analysis of interior permanent magnet synchronous motors by considering mechanical stress and deformation of stators and rotors. *IEEE Transactions on Magnetics*, 2014, 50(2): 7022504-1-7022504-4.

[11] K Yamazaki, M Kumagai, T Ikemi, et al. A novel rotor design of interior permanent-magnet synchronous motors to cope with both maximum torque and iron-loss reduction. *IEEE Transactions on Industry Applications*, 2013, 49(6): 2478-2486.

[12] H Toda, K Senda, M Ishida. Effect of material properties on motor iron loss in PM brushless dc motor. *IEEE Transactions on Magnetics*, 2005, 41(10): 3937-3939.

[13] C P Steinmetz. On the law of hysteresis. *Transactions of the American Institute of Electrical Engineers*, 1892, 9 (1): 1-64.

[14] G Bertotti. General properties of power losses in soft ferromagnetic materials. *IEEE Transactions on Magnetics*, 1988, 24(1): 621-630.

[15] A Boglietti, A Cavagnino, M Lazzari. Predicting iron losses in soft magnetic materials with arbitrary voltage supply: an engineering approach. *IEEE Transactions on Magnetics*, 2003, 39(2): 981-989.

[16] A Boglietti, A Cavagnino, M Lazzari. Fast method for the iron loss prediction in inverter-fed induction motors. *IEEE Transactions on Industry Applications*, 2010, 46(2): 806-811.

[17] M Popescu, D M Ionel, A Boglietti, et al. A general model for estimating the laminated steel losses under PWM voltage supply. *IEEE Transactions on Industry Applications*, 2010, 46(4): 1389-1396.

[18] H S Zhao, D D Zhang, Y L Wang, et al. Piecewise variable parameter loss model of laminated steel and its application in fine analysis of iron loss of inverter-fed induction motors. *IEEE Transactions on Industry Applications*, 2018, 54(1): 832-840.

[19] J Reinert, A Brockmeyer, R D Doncker. Calculation of losses in ferro- and ferrimagnetic materials based on the modified Steinmetz equation. *IEEE Transactions on Industry Applications*, 2001, 37(4): 1055-1061.

[20] E Barbisio, F Fiorillo, C Ragusa. Predicting loss in magnetic steels under arbitrary induction waveform and with minor hysteresis loops. *IEEE Transactions on Magnetics*, 2004, 40(4): 1810-1819.

[21] H Yoon, M Song, I Kim, et al. Accuracy improved dynamic E&S vector hysteresis model and its application to analysis of iron loss distribution in a three-phase induction motor. *IEEE Transactions on Magnetics*, 2012, 48(2): 887-890.

[22] M Song, H Yoon, H Yang, et al. A generalized Chua-type vector hysteresis model for both the non-oriented and grain-oriented electrical steel sheets. *IEEE Transactions on Magnetics*, 2011, 47(5): 1146-1149.

[23] Y L Zhang, Y H Eum, D X Xie, et al. An improved engineering model of vector magnetic properties of grain-oriented electrical steels. *IEEE Transactions on Magnetics*, 2008, 44(11): 3181-3184.

[24] D Kowal, P Sergeant, L Dupré, et al. Comparison of iron loss models for electrical machines with different frequency domain and time domain methods for excess loss prediction. *IEEE Transactions on Magnetics*, 2015, 51(1): 6300110-1-6300110-10.

[25] N Denis, M Inoue, K Fujisaki, et al. Iron loss reduction in permanent magnet synchronous motor by using stator core made of nanocrystalline magnetic material. *IEEE Transactions on Magnetics*, 2017, 53(11): 8110006-1-8110006-6.

[26] Y Miyama, M Hazeyama, S Hanioka, et al. PWM carrier harmonic iron loss reduction technique of permanent-magnet motors for electric vehicles. *IEEE Transactions on Industry Applications,* 2016, 52(4): 2865-2871.

[27] S W Hwang, M S Lim, J P Hong. Hysteresis torque estimation method based on iron-loss analysis for permanent magnet synchronous motor. *IEEE Transactions on Magnetics*, 2016, 52(7): 8204904-1-8204904-4.

[28] M S Lim, S H Chai, J P Hong. Design and iron loss analysis of sensorless-controlled interior permanent magnet synchronous motors with concentrated winding. *IET Electr. Power Appl.*, 2014, 8(9): 349-356.

[29] M Oka, T Ogasawara, N Kawano, et al. Estimation of suppressed iron loss by stress-relief annealing in an actual induction motor stator core by using the excitation inner core method. *IEEE Transactions on Magnetics,* 2014, 51(11): 8202904-1-8202904-4.

[30] F Chai, P X Liang, Y L Pei, et al. Analytical method for iron losses reduction in interior permanent magnet synchronous motor. *IEEE Transactions on Magnetics*, 2015, 51(11): 6301404-1-6301404-4.

[31] M Barcaro, N Bianchi, F Magnussen. Rotor flux-barrier geometry design to reduce stator iron losses in synchronous IPM motors under FW operations. *IEEE Transactions on Industry Applications*, 2010, 46(5): 1950-1958.

[32] F L Fu, X G Tang. *Design handbook of induction motors.* Beijing: China Machine Press, 2006. (in Chinese)

[33] L Lü, W L Xiong. The analysis of electromagnetic design and dynamic characteristics of high-frequency motorized spindle motors based on inverter supply. *Computer Software Copyright*, China, No.2010SR007969. (in Chinese)

[34] D M Ionel, M Popescu, M I McGilp, et al. Computation of core losses in electrical machines using improved models for laminated steel. *IEEE Transactions on Industry Applications*, 2007, 43(6): 1544-1564.

[35] L Aarniovuori, P Rasilo, M Niemelä, et al. Analysis of 37-kW converter-fed induction motor losses. *IEEE Transactions on Industrial Electronics*, 2016, 63(9): 5357-5365.

Biographical notes

Lang Lü, born in 1977, is currently a lecturer at *College of Mechanical Engineering, Hunan Institute of Engineering, China*. He received his PhD degree from *Hunan University, China,* in 2010. His main research interests include motorized spindle system dynamics, the electromagnetic design and analysis of spindle motors as well as high speed and high power electrical

machines.
Tel: +86-0731-58683909; E-mail: 562035363@qq.com

Wan-Li Xiong, born in 1971, is currently a professor and PhD candidate supervisor at *National Engineering Research Center for High Efficiency Grinding*, *Hunan University*, *China*. He received his PhD degree from *Northeastern University*, *China*, in 2000. His research interests include high performance machine tool spindles.
Tel: +86-0731-88821895; E-mail: wan369@vip.sina.com

Can Hu, born in 1987, is currently a lecturer at *School of Mechanical Engineering, Hunan University of Science and Technology*, *China*. He received his PhD degree from *Hunan University*, *China*, in 2019. His research interests include high performance machine tool spindles.
Tel: +86-0731-58290847; E-mail: c_hu86@foxmail.com